FUNCTIONAL GENE EXPRESSION PROFILING IN YEAST IMPLICATES TRANSLATIONAL DYSFUNCTION IN MUTANT HUNTINGTIN TOXICITY

Eran Tauber[1*], Leonor Miller-Fleming[1,2*], Robert P. Mason[1*], Wanda Kwan[3], Jannine Clapp[1], Nicola J. Butler[1], Tiago F. Outeiro[2,4], Paul J. Muchowski[3], and Flaviano Giorgini[1]

[1]Department of Genetics, University of Leicester, Leicester LE1 7RH, UK, [2]Cell and Molecular Neuroscience Unit, Instituto de Medicina Molecular, Av. Prof. Egas Moniz, 1649-028, Lisboa, Portugal, [3]Gladstone Institute of Neurological Disease, Departments of Biochemistry and Biophysics, and Neurology, University of California, San Francisco, California, 94158, USA, [4]Instituto de Fisiologia, Faculdade de Medicina da Universidade de Lisboa, Av. Prof. Egas Moniz, 1649-028 Lisboa, Portugal

*Contributed equally to the work.

Running head: Functional profiling of mutant huntingtin toxicity in yeast

Address correspondence to: Flaviano Giorgini, University of Leicester, Department of Genetics, University Road, Leicester, LE2 3YD, UK. Phone: 44 (0)116 252 3485; Fax: 44 (0)116 252 3378; E-mail: fg36@le.ac.uk.

Huntington's disease (HD) is a neurodegenerative disorder caused by the expansion of a polyglutamine tract in the huntingtin (htt) protein. To uncover candidate therapeutic targets and networks involved in pathogenesis we integrated gene expression profiling and functional genetic screening to identify genes critical for mutant htt toxicity in yeast. Using mRNA profiling we have identified genes differentially expressed in wild-type yeast in response to mutant htt toxicity, as well as in three toxicity suppressor strains: *bna4*Δ, *mbf1*Δ, and *ume1*Δ. *BNA4* encodes the yeast homolog of kynurenine 3-monooxygenase (KMO), a promising drug target for HD. Intriguingly, despite playing diverse cellular roles, these three suppressors share common differentially expressed genes involved in stress response, translation elongation, and mitochondrial transport. We then systematically tested the ability of the differentially expressed genes to suppress mutant htt toxicity when overexpressed, and have thereby identified 12 novel suppressors, including genes that play a role in stress response, Golgi to endosome transport, and rRNA processing. Integrating the mRNA profiling data and the genetic screening data we have generated a robust network which shows enrichment in genes involved in rRNA processing and ribosome biogenesis. Strikingly, these observations implicate dysfunction of translation in the pathology of HD. Recent work has shown that regulation of translation is critical for lifespan extension in *Drosophila* and that manipulation of this process is protective in Parkinson's disease models. In total these observations suggest that pharmacological manipulation of translation may have therapeutic value in HD.

The fatal neurodegenerative disorder Huntington's disease (HD) is characterised by involuntary movements, psychological abnormalities, and cognitive dysfunction. A central pathological hallmark of the disease is the selective loss of medium spiny neurons in the striatum of HD patients. HD is a gain-of-function disease caused by the expansion of a CAG repeat in the *IT-15* gene, which encodes a polyglutamine (polyQ) tract in the huntingtin (htt) protein(1). The CAG repeat number is polymorphic in the general population with repeat length ranging from 6 to 35, while individuals affected by HD have a repeat length of greater than 35. The length of the polyQ expansion in htt correlates directly with kinetics of its aggregation *in vitro* and with severity of the disease in HD patients, and indirectly with age of onset(2). Though increased size of the triplet repeat expansion correlates to an earlier age of onset, there is great variability in the age of onset of HD, even when controlling for repeat length. Indeed, a study by the U.S.-Venezuela Collaborative Research Project with HD kindreds containing over 18,000 individuals has found that approximately 40% of variation in age of onset at controlled repeat lengths is due to genetic modifiers(3), suggesting that many therapeutic targets may be available for treating progression of this devastating disorder.

Since the cloning of the HD disease gene in 1993, several transgenic models of HD have been generated in a variety of organisms, including yeast, *C. elegans*, *Drosophila*, and mice. These

models have allowed researchers to explore the underlying mechanisms of HD pathogenesis, as well as to perform genetic screens and to test candidate therapeutic compounds. Yeast models have proven to be particularly powerful and facile for high-throughput approaches as well as for molecular genetic manipulations(4). While not all aspects of pathogenesis can be studied in a single-cell organism like yeast, expression of a mutant htt fragment in yeast produces several HD-relevant phenotypes such as formation of mutant htt-containing aggregates, transcriptional dysregulation, cellular toxicity, perturbations in kynurenine pathway metabolites, increased levels of reactive oxygen species (ROS), mitochondrial dysfunction, defects in endocytosis, and apoptotic events(5).

In a genome-wide screen we identified 28 gene deletions that suppress toxicity of a mutant htt fragment (Htt103Q) in yeast(6). We focus on three of these suppressor genes in this study: *BNA4*, *MBF1*, and *UME1*. *BNA4* encodes the yeast homolog of the mammalian enzyme kynurenine 3-mononygenase (KMO), which catalyzes the hydroxylation of kynurenine in the kynurenine pathway of tryptophan degradation(7). Increased levels of two neurotoxic kynurenine pathway metabolites downstream of KMO have been implicated in the pathophysiology of HD: 3-hydroxykynurenine (3-HK) and quinolinic acid (QUIN)(8). The kynurenine pathway metabolites and enzymes are well conserved between yeast and humans, and the genetics of the pathway has been extensively characterized in yeast(7). We have dissected this pathway in yeast with regards to its influence on mutant htt toxicity, and found that much like in HD patients the levels of 3-HK and QUIN are increased in cells expressing a toxic mutant htt fragment(6,9). Importantly, we found that lowering levels of these metabolites in yeast by genetic or pharmacological inhibition of Bna4 ameliorates disease-relevant phenotypes.

Ume1 is a component of the Rpd3 histone deacetylase (HDAC) complex in yeast. Several studies in fly and mouse models of HD have shown that inhibition of HDAC function either pharmacologically or genetically ameliorates HD-relevant phenotypes(10). In addition, we have found that HDAC inhibitors decrease levels of 3-HK and KMO activity in R6/2 HD model mice and in primary microglia cultured from these animals(8). Ume1 is required for full transcriptional repression of a subset of genes in yeast, in a mechanism requiring Rpd3 and Sin3(11), suggesting that genetic inhibition of the yeast Rpd3 HDAC complex relieves polyQ toxicity in a mechanism similar to that observed in fly and mouse polyQ disease models. We have previously found that in *ume1*Δ cells expressing Htt103Q both kynurenine pathway genes (*BNA1*, *BNA2*, *BNA4*, *BNA5*) and kynurenine pathway metabolites (3-HK and QUIN) are downregulated as compared to wild-type cells expressing the same construct(8). Interestingly, we also found that the genes down-regulated in wild-type cells expressing Htt103Q cells are enriched for Rpd3-target genes. These observations directly link transcriptional dysregulation and perturbations in the kynurenine pathway in HD(8).

MBF1 encodes a transcriptional coactivator conserved from yeast to humans that bridges the DNA-binding region of transcriptional activator Gcn4 and TATA-binding protein (TBP) Spt15, a general transcription factor required for transcription by the three nuclear RNA polymerases (I, II, III)(12,13). Interestingly, a polyQ expansion in TBP in humans leads to Spinocerebellar ataxia 17, which in many patients has phenotypes indistinguishable from HD(14). Gcn4 is considered to be the master regulator of amino acid metabolism in yeast. It is a member of the AP-1 family of transcription factors, and regulates the expression of genes involved in 19 out of 20 amino acid biosynthetic pathways, purine biosynthesis, autophagy (*APG1*, *APG13*, *APG14*), and multiple stress responses(15). In addition, it has been observed that ~90 *RPL* (Ribosomal Protein, Large subunit) and *RPS* (Ribosomal Protein, Small subunit) genes which encode ribosomal proteins are repressed by activation of Gcn4 under stress conditions(15).

Here we expand on our previous studies by using a unique combination of functional approaches and differential gene expression analysis on a genome-wide scale. In order to identify critical genes/pathways/networks involved in suppression of mutant htt toxicity, we employ oligonucleotide microarray analysis to identify genes differentially expressed in mutant htt expressing cells compared to controls, as well as in three suppressor deletion strains expressing a toxic mutant htt fragment: *bna4*Δ, *mbf1*Δ, and

*ume1*Δ. We next functionally interrogate 380 of these differentially expressed genes (DEGs) by testing the effect of overexpression of the respective ORFs on mutant htt toxicity in yeast, and thereby identify 14 DEGs that modulate mutant htt toxicity. In total this work identifies ribosomal biogenesis and rRNA processing as critical cellular processes modulated in eukaryotic cells expressing a mutant htt fragment, which suggests these processes are likely relevant to HD pathophysiology and therapy.

EXPERIMENTAL PROCEDURES

Yeast strains and DNA constructs - The strains used for microarray experiments were from the yeast gene deletion set in the MATa (BY4741) [*MAT***a** *his3*Δ1 *leu2*Δ0 *met15*Δ0 *ura3*Δ0] strain background (Open Biosystems). The Y258 strain background [*MAT***a** *pep*4-3, *his*4-580, *ura*3-53, *leu*2-3,112] was used for the overexpression studies (Open Biosystems). The constructs pYES2-Htt25Q-GFP and pYES2-Htt103Q-GFP(16) were used for the microarray studies. Htt103Q is a galactose (GAL)-inducible, FLAG- and GFP-tagged construct encoding the first 17 amino acids of Htt fused to a polyQ tract of 103 glutamines. The constructs p425*GALL*-Htt25Q-GFP and p425*GALL*-Htt103Q-GFP were used in the yeast overexpression studies and were generated by amplifying the huntingtin constructs from pYES2-Htt25Q-GFP and pYES2-Htt103Q-GFP and cloning into the *Spe*I and *Xho*I sites of p425*GALL*(17).

Yeast total RNA preparation - SC –Ura galactose (2%) cultures (12 ml) were inoculated at OD_{600} 0.2 and incubated with shaking at 30º C until reaching an OD_{600} of ~1.0. Cells were harvested and lysed with acid-washed glass beads. Total RNA was isolated with Qiagen RNeasy Midi kits, following standard protocols.

Gene expression analysis by DNA oligonucleotide arrays - Double-stranded cDNA was synthesized from total RNA, amplified as cRNA, labeled with biotin, and hybridized to Affymetrix Yeast Genome S98 Array GeneChips, which were washed and scanned at the University of Washington Center for Expression Arrays and at the J. David Gladstone Institutes Genomics Core Laboratory, University of California, San Francisco according to manufacturer protocols. Images were processed with Affymetrix Microarray Suite 5.0 (MAS-5). The quality of hybridization and overall chip performance were determined from the MAS-5 generated report file.

Analysis of Microarray Data - The statistical computing language R(18) was used for quality controls, pre-processing and analyses of the data. The quality of the microarrays was assessed by inspecting pseudo-images of the arrays, MA scatter plots of the arrays versus a pseudo-median reference chip, and histogram and boxplot of raw log intensities, and relative log expressions. Expression data are available through the Gene Expression Omnibus (GEO) database, accession number GSE18644. The data were analysed using the R bioconductor package affylmGUI (version 1.8.0), the graphic interface to limma (version 2.9.17)(19). Data were normalized and summarised using the GCRMA method(20). DEGs were identified by using a moderated t-test (limma). To correct for multiple comparison we have estimated the false-discovery rate (FDR) using the QVALUE package(21) with a typical FDR threshold (q) of 10%. Gene ontology searches were performed with the Functional Annotation Tool (http://david.abcc.ncifcrf.gov/home.jsp). Network visualization was performed using the Osprey Network Visualization System (Version 1.2.0), which is powered by the BioGRID database (http://www.thebiogrid.org)(22). Cis-regulatory elements of the DEGs were identified using the MUSA algorithm(23) in the YEASTRACT suite(24). The Position Weight Matrix of each family was used to search for known transcription factor binding sites in the YEASTRACT database using the Smith-Waterman local alignment algorithm (using the sum of the squared distances metric).

Real-Time Quantitative PCR - The BY4741 yeast strain was transformed independently with pYES2-Htt103Q-GFP and pYES2-Htt25Q(16) by standard procedures. Yeast cells were grown overnight in complete media lacking uracil (SC-URA) containing glucose (2%) as a carbon source. Cultures were diluted back to optical density 0.4 and grown in SC-URA containing galactose (2%) to induce protein expression. Cells were harvested after growing 25 hours, pelleted and stored at -80ºC until needed. RNA was extracted using the Qiagen RNeasy Midi kits following manufacturer instructions. Genomic DNA contamination was

removed from RNA using Turbo DNAse according to the manufacturer's protocol. 500 ng of RNA was used as a template to synthesize cDNA with the Qiagen QuantiTect® Reverse Transcription kit. To ensure that RNA had no genomic DNA contamination a control reaction was included in which no reverse transcription was carried out. 17 genes were selected to analyse the mRNA expression levels by quantitative PCR and actin-1 was chosen as a reference. Reactions were carried out in a LightCycler Real-Time PCR System (Roche). cDNA was quantified using 5 ul of Sybr Green (Fermentas) and 0.3 uM of forward and reverse primers. Primers were analyzed for specificity and efficiency by melting curve analysis. The efficiency was calculated at the end of each amplification reaction via relative standard curves. PCR efficiencies ranged from 0.80 to 1.0. Standard curves were calculated using the amplification of 5 serial dilutions of genomic DNA in triplicate. At least three independent cDNA samples were analysed. PCR reactions were run in duplicate. Relative quantification was performed using LightCycler® 480 Relative Quantification Software. The crossing points were calculated by the second derivative method and relative expression was calculated by the available advanced relative quantification. Further analysis and statistical tests were performed using the Relative Expression Software 2008 (REST)(25,26). The relative quantification was corrected for PCR efficiency via both methods.

Functional Testing of DEGs - Yeast strains containing plasmids for the overexpression of selected genes were obtained from the yeast ORF collection in the Y258 strain background. The relevant yeast strains were grown overnight in 96 well plates containing 100 µl of SC-URA supplemented with 2% glucose per well and transformed with either p425*GALL*-Htt25Q-GFP or p425*GALL*-Htt103Q-GFP using a high throughput transformation method(4). Transformants were grown to stationary phase in complete media lacking uracil and leucine (SC–Ura–Leu) containing 2% glucose, serial diluted, and spotted onto SC-Ura-Leu media supplemented with either 2% glucose or 2% galactose and 2% raffinose. Plates were incubated at 30˚C for 3-5 days and yeast strains scored for growth.

Determination of RNQ prion status - 20 ml cultures of suppressor strains were grown to approximately an OD_{600} 1.0 in SC –Ura GAL/RAF media, at which point cells were harvested by centrifugation at 3000 rpm for 5 min. Cell pellets were washed with 10 ml water and spun as above. The cell pellets were resuspended in 200 µl lysis buffer (100 mM Tris pH 7.0, 200 mM NaCl, 1mM EDTA, 5% glycerol, 0.5 mM DTT, 1X protease inhibitor cocktail) and transferred to microfuge tubes. The cells were lysed by addition of ~200 µl of acid washed glass beads (425-600 µm, Sigma, St. Louis, MO), vortexing for 1 min, addition of 200 µl of RIPA buffer (50 mM Tris pH 7.0, 200 mM NaCl, 1% Triton, 0.5 % Na-deoxycholate, 0.1% SDS), and further vortexing for 10 sec. Samples were then centrifuged at 3000 rpm for 15 sec to pellet the glass beads and cell debris. 60 µl of supernatant was used as the "Total" sample, while 200 µl of the supernatant was centrifuged for 30 min at 80,000 rpm in the Beckman TLA 100 Ultracentrifuge. 60 µl of the supernatant from this step was isolated and used at the "Soluble" fraction, while the "Pellet" fraction was prepared by resuspending the pellet in 100 µl of lysis buffer and 100 µl of RIPA buffer, adding 67 µl of 4X protein sample buffer (SB), and boiling for 5 minutes. 20 µl of 4X SB was added to the "Total" and "Soluble" fractions, and boiled for 5 min. The samples were resolved by SDS-PAGE and immunoblotting as described above. Curing yeast strains of endogenous prion cells was performed by growth for 5 passages on YPD supplemented with 5 mM guanidine hydrochloride (GuHCl) (27).

RESULTS

Yeast expressing a mutant htt fragment differentially express genes involved in ribosome biogenesis and rRNA processing. We recently performed oligonucleotide microarray hybridization assays to compare mRNA expression profiles of isogenic parental yeast (BY4741, MAT a) expressing either a wild-type or mutant htt fragment (Htt25Q or Htt103Q, respectively)(9). Here we re-analysed the data from this experiment using the limma package implemented in R/Bioconductor(19,28).This analysis showed that in Htt103Q-expressing cells, expression of 226 genes was up-regulated when compared to Htt25Q-expressing cells, whereas expression of 244 genes was down-regulated (q value < 0.2) (Figure 1A). A

subset of these DEGs were analysed and confirmed via quantitative real-time PCR (QPCR)(Table S1).

We used the DAVID Bioinformatics Resources Functional Annotation Tool (http://david.abcc.ncifcrf.gov) to test whether the DEGs were enriched by known or predicted function using gene ontology (GO)(29). In a manner similar to our previous analysis, functional groups up-regulated significantly in the Htt103Q expressing cells included genes involved in protein folding ($P < 1.0 \times 10^{-3}$) and response to stress ($P < 0.01$)(Table S2)(9). In addition, the new analysis found enrichment in the GO terms of response to unfolded protein ($P < 1.0 \times 10^{-5}$), ubiquitin cycle ($P < 0.01$), post-translational protein modification ($P < 0.01$), and vacuolar protein catabolic process ($P < 0.05$). We previously described that down-regulated genes in Htt103Q-expressing cells were involved in the functional groups of ribosome biogenesis ($P < 1.0 \times 10^{-39}$) and rRNA processing and metabolism ($P < 1.0 \times 10^{-20}$)(9), and we have confirmed those observations in our new analyses (Table S3). These data suggest that yeast cells expressing Htt103Q mount a response to deal with this toxic, misfolded protein, via upregulation of proteins involved with protein misfolding, protein degradation, autophagy, and stress response. At the same time, in a manner similar to classic heat shock response, the presence of Htt103Q in yeast cells causes a dramatic reduction in expression of genes involved in rRNA metabolism and ribosome biogenesis, suggesting that general protein synthesis in these cells is significantly repressed, ultimately contributing to Htt103Q-dependent toxicity.

Common mechanisms underlie mutant htt toxicity suppression in gene deletion suppressor strains. In order to discern if there are common mechanisms underlying toxicity suppression in mutant htt suppressor strains, we wished to next monitor gene expression perturbations in three gene deletion Htt103Q suppressor strains: *bna4*Δ, *mbf1*Δ, and *ume1*Δ(6). Thus, we performed microarray experiments to identify DEGs in *bna4*Δ, *mbf1*Δ, or *ume1*Δ yeast expressing Htt103Q versus parental wild-type cells expressing Htt103Q. We tested the 200 DEGs which showed the highest fold change (and $q < 0.1$) from each deletion suppressor for enrichment of GO terms. We found that in *bna4*Δcells expressing Htt103Q there is an enrichment of several GO terms as compared to control cells, including carboxylic acid metabolism ($P < 1.0 \times 10^{-4}$), translation elongation ($P < 1.0 \times 10^{-3}$), nitrogen compound metabolism ($P < 1.0 \times 10^{-3}$), water-soluble vitamin biosynthesis ($P < 0.01$), and vesicle organization and biogenesis ($P < 0.05$)(Table S4). DEGs in *mbf1*Δ cells showed enrichment in many GO term categories, including amino acid metabolism ($P < 1.0 \times 10^{-11}$), nitrogen compound metabolism ($P < 1.0 \times 10^{-9}$), carboxylic acid metabolism ($P < 1.0 \times 10^{-7}$), and urea cycle intermediate metabolic process ($P < 1.0 \times 10^{-4}$) (Table S5). The *ume1*Δ suppressor strain exhibited DEGs with enrichment in GO term categories of water-soluble vitamin biosynthesis ($P < 0.01$), NAD biosynthesis ($P < 0.01$), nitrogen compound metabolism ($P < 0.01$), carboxylic acid metabolism ($P < 0.05$), among others (Table S6). The four genes present within the NAD biosynthesis GO group are the central kynurenine pathway genes of *BNA1*, *BNA2*, *BNA4*, and *BNA5*, confirming our original analysis with this data set(8). It is critical to note that while some of the GO groups enriched in these data are specific to individual suppressors, several categories are common amongst these suppressors, such as nitrogen compound metabolism and carboxylic acid metabolism.

As full levels of Htt103Q toxicity are dependent upon the presence of the Rnq1 yeast prion [RNQ^+](16), we analysed Rnq1 prion status in the three gene deletion strains to ensure that the DEGs identified above are independent of Rnq1 prion. To this end, we analysed Rnq1 by sedimentation analysis in all three suppressor strains (Figure 2A,B). We found that in all three strains Rnq1 was present in the pellet fraction of cells expressing Htt103Q or carrying empty vector (pYES2), indicating that Rnq1 is present in its prion form independent of Htt103Q expression. Interestingly, in the case of the *bna4*Δ strain, we observed that Rnq1 is also present in the soluble fraction, suggesting that this population of cells contains both prion and non-prion forms of Rnq1 (Figure 2B). A similar phenotype has been described with other deletion strains from this library(30). Treatment with the prion curing agent GuHCl shifted Rnq1 from the pellet fraction to the soluble fraction, providing further support that Rnq1 status is "mixed" in the *bna4*Δ strain (Figure 2B). To test whether prion status was directly

altered by the deletion of *BNA4* we analyzed a second *bna4*Δ strain, and consistent with previously published work(30), we found that Rnq1 was entirely in prion form, indicating that the "mixed" prion phenotype is independent of *BNA4* deletion (Figure 2C). In total this data suggests that DEGs identified in the *mbf1*Δ and *ume1*Δ strains are independent of Rnq1 prion status, while a subset of DEGs from the BY4741 *bna4*Δ strain may arise from [RNQ^+]-dependent modulation of Htt103Q.

In order to filter out DEGs dependent upon modulation of Rnq1 prion status, and to ascertain if common genes/mechanisms underlie suppression in the three suppressor strains, we cross-compared the three sets of DEGs identified above (Figure 1B). Strikingly, we found that 15 annotated genes were common among these three groups, seven of which are also differentially expressed in WT cells expressing Htt103Q (Table 1). Assuming independence, the probability of finding 15 genes shared amongst these three groups is $< 1.0 \times 10^{-13}$, which supports the notion that the suppressors share common mechanisms of mutant htt suppression. The genes shared among the suppressor strains function in a variety of cellular processes, including translation elongation (*ANB1*), stress response (*DAK2*), amino acid transport (*DIP5*), lactate metabolism (*DLD3*), and mitochondrial transport (*YMC2*). Interestingly, 3 of the 15 genes are predicted to encode tRNAs, all of which are down-regulated in the suppressor strains. Of these genes, 2 encode tRNAs for tRNA-Pro and one encodes tRNA-Lys (Table 1). In 13/15 cases the genes are differentially expressed in the same direction in all three suppressor strains, reinforcing the notion that the shared DEGs represent common underlying mechanisms involved in mutant htt toxicity. Intriguingly, of these 13 genes, 5 are differentially expressed in the opposite direction in Htt103Q-expressing cells (*AQR1*, *DAK2*, *YGR035C*, *YMC2*, *YOR338W*)(Table 1 and Table S7).

This observation led us to compare the overlapping DEGs from the individual suppressor strains to the top 200 DEGs from Htt103Q expressing cells to ascertain if a negative correlation exists in expression between these groups of DEGs. Strikingly, in all three comparisons we found a significant negative correlation in differential expression of the overlapping genes (Figure 1C). This suggests that the differential expression observed in the parental WT strain due to expression of Htt103Q is relieved in the three deletion suppressor strains. Though it is likely that these changes in expression profiles directly contribute to mutant htt toxicity, we cannot exclude the possibility that the changes are simply a downstream consequence of cellular toxicity.

Cis-regulatory domain analysis of DEGs identifies enriched elements. To clarify whether common regulatory mechanisms were affected in Htt103Q-expressing cells as compared to Htt25Q controls, the DEGs with local false discovery rate (FDR) < 2%, as estimated by the Rank product algorithm (n=46), were analysed for shared regulatory motifs using the MUSA algorithm. This analysis revealed 14 families of *de novo* motifs that were significantly over-represented in these sequences(23)(Table 2). Aligning the Position Weight Matrix (PWM) of each family with the PWM of known transcription factors revealed several matches. Interestingly, Gcn4 was among the transcription factors identified, suggesting a link between response to Htt103Q-dependent toxicity and this transcription factor. The list of transcription factors identified includes several zinc transcription factors such as Hap1 (which responds to heme and oxygen levels), Azf1 (responds to glucose) and Zap1 (responds to zinc levels). Other candidate transcription factors include Cup2, a copper-binding transcription factor which responds to copper levels, and Ime1, which is the master regulator of meiosis, and activates early meiotic genes through interactions with Ume6(31), another transcription factor whose binding site was over-represented in the DEGs (Table 2). Ume6 recruits the Rpd3-Sin3 HDAC complex during mitosis to repress early meiosis-specific genes via hypoacetylation of histones H3 and H4(32). Critically, Ume6 has been shown by affinity mass spectrometry to be a component of the Rpd3-Sin3 corepressor complex along with the loss-of-function Htt103Q suppressors Ume1 and Rxt3(6,33). Thus, this observation further implicates transcriptional dysregulation in mutant htt toxicity and HDACs as candidate therapeutic targets.

A unique subset of differential expressed, highly interconnected genes modulate mutant htt toxicity. In order to ascertain the potential role of

the DEGs in mutant htt toxicity, we individually tested the ability of these genes to suppress toxicity of Htt103Q when individually overexpressed in yeast. All of the genes that were available as open reading frame (ORF) constructs from the Yeast ORF Collection (380/470, 80.9%) were individually tested via growth assays for suppression of Htt103Q toxicity. We found that 12 of the DEGs suppressed toxicity of Htt103Q when overexpressed (Figure 3, Table 3). To eliminate the possibility that the DEGs suppressed toxicity by silencing Htt103Q expression, we analyzed expression levels by Western and dot blotting, and found that Htt103Q expression was unchanged (Figure S1A,B). In addition, we confirmed that Rnq1 remains in its prion conformation when expression of a DEG is induced (Figure S1C).

Interestingly, these overexpression suppressors include genes whose expression is upregulated as well as genes whose expression is downregulated in cells expressing Htt103Q, indicating two different models for overexpression protection: 1) ORF overexpression mimics upregulation of genes exerting a protective role against mutant htt toxicity, or 2) ORF overexpression is rescuing a depletion of a critical factor (Table 3). Excitingly, these overexpression suppressors are potential candidate therapeutic targets for HD. Of the 12 novel suppressors, 7 (~ 58%) have human orthologs as determined by Ensembl Genome Browser (http://www.emsembl.org).

We next compared our list of DEGs with our previously published gene deletion enhancers and suppressors of mutant htt toxicity, and identified another two common genes (*MBF1*, *APJ1*)(6,34). Thus, in total we identified 14 DEGs that modify mutant htt toxicity when overexpressed or deleted (Table 3). Amongst these 14 genes, we observed enrichment of genes within seemingly unrelated functional groups. In particular, this group was enriched for genes involved in rRNA processing (*BUD23*, *DBP2, IPI3, NSA2*, *RRP9, UTP9*), stress/heat shock response (*APJ1*, *JJJ3*), and transcription (*CSE2* and *MBF1*) (Table 3). Interestingly, aside from rRNA processing, all of these functional groups have been extensively implicated in HD pathology.

To clarify the functional connectivity amongst this functionally validated list of DEGs we performed network analysis using the Osprey Network Visualization System (Version 1.2.0), which allows visualization of complex interaction networks(22). This software is powered by the BioGRID database (http://www.thebiogrid.org), which houses and distributes data collections of protein and genetic interactions of model organisms, including yeast via the *Saccharomyces* Genome Database (http://www.yeastgenome.org). Via these databases, Osprey allows insertion of all known interactions for each "node" (gene of interest). The interactions types (or "edges") include data from affinity capture experiments, two-hybrid screens, and synthetic lethality analyses, among others. Here, we have used Osprey to investigate all the known genetic and physical interactions of the 14 functionally validated DEGs. As an initial test, we asked for all the interactions within these 14 nodes. Interestingly, we found only one interaction amongst these nodes, a physical interaction between Rrp9 and Utp9, both of which are components of the small ribosomal subunit (SSU) processome involved in pre-rRNA processing, as determined by affinity capture/mass spectroscopy studies(35-37) (data not shown). This result highlights our observations from the GO analysis that showed an enrichment in genes from disparate functional groups. In order to determine if the above 14 genes function indirectly in the same network, we explored all of the interactions for these functionally validated nodes, and we found a total of 538 interactions among 464 nodes (data not shown). In order to select genes with higher level relationships, we processed the network data with an iterative minimum filter of two, which identified all of the nodes within this group which have a minimum of two interactions with other genes within the group, and then sorted the remaining nodes by GO function (Figure 4). This analysis uncovered a highly interconnected network of genes, which surprisingly included 11/14 of the original functionally validated genes. Critically, this network of 81 nodes (with 156 edges) reinforced and expanded the GO groups enriched in the mutant htt toxicity interaction network: ribosome biogenesis and assembly (71.6%, $P = 1.2 \times 10^{-49}$), rRNA processing (55.6%, $P = 4.7 \times 10^{-43}$), nuclear transport (12.3%, $P = 1.5 \times 10^{-4}$), and G-protein signalling (2.5%, $P = 4.5 \times 10^{-2}$). When a more stringent iterative minimum filter of three is applied, 5/14 modifiers are still present in the

network (11 nodes; 23 edges), all of which are involved in ribosome biogenesis and assembly ($P = 2.6 \times 10^{-12}$), rRNA processing ($P = 1.2 \times 10^{-8}$), and related processes (data not shown). In total, this work suggests that though these modifiers of mutant htt toxicity play roles in disparate functional groups, they function within a highly-interrelated network.

DISCUSSION

In this study we utilized a novel functional approach to gene profiling experiments in order to dissect the underlying mechanisms of mutant htt toxicity in yeast. This work has not only highlighted the central role of rRNA processing and ribosome biogenesis in mutant htt toxicity in yeast, but has also identified several novel suppressors of this toxicity which are candidate therapeutic targets for HD. Several gene profiling experiments with mammalian models of HD support our observations. Gene expression profiling in PC12 cells and rat striatal cells expressing mutant htt fragments has found an enrichment in genes encoding ribosomal proteins and RNA processing proteins(38,39). In addition, analysis of gene expression in the striatum of R6/2 HD model mice has found an enrichment in genes encoding ribosomal proteins as compared to wild-type controls(40). Recently, microarray profiling using a primary rat neuron model of HD found enrichment in genes involved in RNA splicing/RNA processing(41). Finally, an RNAi screen in *Drosophila* cells identified several modifiers of mutant htt aggregation which play a role in RNA processing(42). In total, these observations suggest that the results described here are not likely to be yeast-specific, but may reflect cellular perturbations conserved in mammalian cells. In addition, in this study we identified DEGs from *bna4*Δ, *mbf1*Δ, and *ume1*Δ strains expressing Htt103Q versus control cells to learn more about underlying mechanisms contributing to Htt103Q toxicity suppression. Analysis of prion status in these strains found that in the *bna4*Δ strain Rnq1 is present in both prion and soluble forms, suggesting that a subset of these DEGs may arise from modulation of [RNQ^+] status. Thus, in order to reduce [RNQ^+]-dependent effects we focused on the cross-section of these DEGs with the DEGs from the *mbf1*Δ and *ume1*Δ strains. By this approach we identified 15 common DEGs amongst these three gene deletion suppressor strains. These genes include 3 tRNA-encoding genes, as well as genes involved in a variety of cellular pathways. What is unclear in the examples above is the mechanism of these changes, and how these changes contribute to mutant htt toxicity, and ultimately to HD pathology. These yeast studies will serve as a strong starting point for future studies elucidating these underlying mechanisms.

A critical finding from this study is the identification of a robust network of interactions derived from 14 differentially expressed genes (nodes) that modulate toxicity of a mutant htt fragment. Despite the original nodes playing roles in diverse cellular processes, the resulting network contains 11 of these nodes within a network of 81 nodes and 156 edges, and has an enrichment of genes involved in rRNA processing and ribosome biogenesis. Intriguingly, several of the functionally validated nodes appear to be highly interconnected in the network (nodes indicated in bold in Figure 4), underscoring the importance of these nodes within the context of the network.

Several of our observations above implicate Gcn4 in mutant htt toxicity in yeast. First, expression of Htt103Q in yeast leads to down-regulation of genes involved in ribosome biogenesis, and under stress conditions Gcn4 is known to repress transcription of ~90 *RPL* and *RPS* genes which encode ribosomal proteins(15). Second, *MBF1*, which is a deletion suppressor of Htt103Q toxicity, encodes a transcriptional coactivator which can bridge Gcn4 and TBP. Third, we found that Gcn4 binding sequences are over-represented in the upstream regions of genes differentially expressed in Htt103Q-expressing cells. In total this work suggests that expression of Htt103Q in yeast may down-regulate expression of ribosomal genes via induction of Gcn4 expression. As Mbf1 expression is required for Gcn4 function, these observations collectively suggest that deletion of *MBF1* may suppress mutant htt toxicity by impairing Gcn4 function. It must also be noted that induction of Gcn4 leads to upregulation of three kynurenine pathway genes, *BNA1* (3-hydroxyanthranilate 3,4-dioxygenase), *BNA4* (which encodes KMO), and *BNA6* (quinolinate phosphoribosyl transferate)(15). Intriguingly, deletions of either *BNA1* or *BNA4* suppresses toxicity of Htt103Q(6). These observations also

support a hypothesis in which Gcn4 induction due to Htt103Q expression contributes to toxicity. We did not, however, see differential expression of *GCN4* in our present study in Htt103Q-expressing cells (data not shown). This is not particularly surprising as *GCN4*, which is under strict transcriptional control, is also under translational control, via four small upstream ORFs (uORFs) in the 5' leader region of the *GCN4* mRNA(43). Induction of translation of the message occurs primarily under environmental stresses(44). In addition, as recruitment of TBP via Mbf1 is the rate-limiting step in Gcn4 activation(12), and *MBF1* expression is upregulated in Htt103Q-expressing yeast (Table 3), it is possible that increased levels of Mbf1 alone may be sufficient to increase Gcn4 activity, without induction of Gcn4 expression. Interestingly, lifespan extension in yeast due to depletion of 60s ribosomal subunits, dietary restriction, or TOR inhibition appears to require induction of Gcn4(45). Thus, in the case of mutant htt expression, Gcn4 induction may reflect a cellular coping mechanism gone awry. This pathway may play a similar role in humans as ATF4, the functional ortholog of Gcn4 in mammals(46), is regulated via a similar translational mechanism and activation of Gcn4 is analogous to the mammalian integrated stress response(47).

In a related note, the yeast eIF4E-associated protein Eap1, which inhibits cap-dependent translation initiation via the TOR signalling cascade, attenuates induction of Gcn4 translation(48). Recent work has shown that overexpression of eIF4E-BP, the Eap1 functional equivalent in *Drosophila*, rescues parkinsonian phenotypes in fly models of Parkinson's disease by inhibiting cap-dependent translation, and thereby inducing expression of genes involved in stress response(49). It has also been seen that during dietary restriction in *Drosophila* 4E-BP promotes lifespan extension by activation of nuclear-encoded mitochondrial protein translation(50).

Interestingly, in the present study we have found that the gene encoding eIF5A, a translation elongation factor, is upregulated in all three suppressor strains expressing Htt103Q, as compared to controls. Taken together, these data suggest that altered regulation of translation may be contributing to mutant htt toxicity, and that pharmacological modulation of this process may have therapeutic relevance. Supporting this, it has been recently shown that rapamycin treatment of mouse embryonic fibroblast cells expressing mutant htt abrogates HD-relevant phenotypes by inhibition of translation, independent of effects on autophagy(51). It is also important to note that while much interest in the HD community has been focused on transcriptional dysregulation in pathogenesis and as a target for therapeutics, our study suggests that the effect of mutant htt on translational processes in the cell may also be critical.

As most basic cellular mechanisms are conserved in yeast to higher eukaryotes, the work presented here will likely inform future studies on disease pathogenesis in HD. Due to the ease and rapidity of genetic screening in yeast, this organism is particularly amenable for integrated approaches to functional gene expression profiling. Yeast will therefore likely provide an important platform for future analyses of disease genes, further evidenced by a recent study dissecting α-synuclein toxicity in yeast(52). It is important to mention that we have identified 12 novel suppressors of mutant htt toxicity in yeast, 7 of which have human orthologs as determined by the Ensembl Genome Browser. Four of these yeast genes (*BUD23*, *ENT3*, *NSA2*, and *RRP9*) have clear 1-to-1 orthologs in humans which could potentially be targeted for therapy if validated in other model systems. Interestingly, *ENT3* has recently been identified as a suppressor of α-synuclein toxicity in yeast(53). In summary, our study has provided new insights into the mechanisms associated with mutant htt toxicity in yeast which may be relevant to HD pathogenesis and has also identified novel candidate targets for therapeutic intervention in this disorder. Clearly it is now critical to test the above hypotheses and to validate the candidate HD targets identified in order to ascertain how our observations are linked to mutant htt toxicity in yeast and how they may inform therapeutic strategies in HD patients. Finally, the power of using yeast to clarify mechanisms involved in HD pathogenesis and to identify candidate drug targets is underscored by our recent validation of KMO as a promising therapeutic target in HD model mice (Zwilling et al., in review).

REFERENCES

1. The Huntington's Disease Collaborative Research Group (1993) *Cell* **72**, 971-983
2. Chen, S., Ferrone, F. A., and Wetzel, R. (2002) *Proc Natl Acad Sci U S A* **99**, 11884-11889
3. Wexler, N. S., Lorimer, J., Porter, J., Gomez, F., Moskowitz, C., Shackell, E., Marder, K., Penchaszadeh, G., Roberts, S. A., Gayan, J., Brocklebank, D., Cherny, S. S., Cardon, L. R., Gray, J., Dlouhy, S. R., Wiktorski, S., Hodes, M. E., Conneally, P. M., Penney, J. B., Gusella, J., Cha, J. H., Irizarry, M., Rosas, D., Hersch, S., Hollingsworth, Z., MacDonald, M., Young, A. B., Andresen, J. M., Housman, D. E., De Young, M. M., Bonilla, E., Stillings, T., Negrette, A., Snodgrass, S. R., Martinez-Jaurrieta, M. D., Ramos-Arroyo, M. A., Bickham, J., Ramos, J. S., Marshall, F., Shoulson, I., Rey, G. J., Feigin, A., Arnheim, N., Acevedo-Cruz, A., Acosta, L., Alvir, J., Fischbeck, K., Thompson, L. M., Young, A., Dure, L., O'Brien, C. J., Paulsen, J., Brickman, A., Krch, D., Peery, S., Hogarth, P., Higgins, D. S., Jr., and Landwehrmeyer, B. (2004) *Proc Natl Acad Sci U S A* **101**, 3498-3503
4. Giorgini, F., and Muchowski, P. J. (2006) *Methods Enzymol* **412**, 201-222
5. Giorgini, F., and Muchowski, P. J. (2009) *Methods Mol Biol* **548**, 161-174
6. Giorgini, F., Guidetti, P., Nguyen, Q., Bennett, S. C., and Muchowski, P. J. (2005) *Nat Genet* **37**, 526-531
7. Panozzo, C., Nawara, M., Suski, C., Kucharczyka, R., Skoneczny, M., Becam, A. M., Rytka, J., and Herbert, C. J. (2002) *FEBS Lett* **517**, 97-102
8. Giorgini, F. (2008) The kynurenine pathway and microglia: Implications for pathology and therapy in Huntington's disease. in *Protein Misfolding in Biology and Disease* (T, O. ed.), Transworld Research Network, Kerala, India. pp 231-255
9. Giorgini, F., Moller, T., Kwan, W., Zwilling, D., Wacker, J. L., Hong, S., Tsai, L. C., Cheah, C. S., Schwarcz, R., Guidetti, P., and Muchowski, P. J. (2008) *J Biol Chem* **283**, 7390-7400
10. Kazantsev, A. G., and Thompson, L. M. (2008) *Nat Rev Drug Discov* **7**, 854-868
11. Mallory, M. J., and Strich, R. (2003) *J Biol Chem* **278**, 44727-44734
12. Takemaru, K., Harashima, S., Ueda, H., and Hirose, S. (1998) *Mol Cell Biol* **18**, 4971-4976
13. Takemaru, K., Li, F. Q., Ueda, H., and Hirose, S. (1997) *Proc Natl Acad Sci U S A* **94**, 7251-7256
14. Stevanin, G., Fujigasaki, H., Lebre, A. S., Camuzat, A., Jeannequin, C., Dode, C., Takahashi, J., San, C., Bellance, R., Brice, A., and Durr, A. (2003) *Brain* **126**, 1599-1603
15. Natarajan, K., Meyer, M. R., Jackson, B. M., Slade, D., Roberts, C., Hinnebusch, A. G., and Marton, M. J. (2001) *Mol Cell Biol* **21**, 4347-4368
16. Meriin, A. B., Zhang, X., He, X., Newnam, G. P., Chernoff, Y. O., and Sherman, M. Y. (2002) *J Cell Biol* **157**, 997-1004
17. Mumberg, D., Muller, R., and Funk, M. (1994) *Nucleic Acids Res* **22**, 5767-5768
18. Team, R. D. C. (2009) R: A Language and Environment for Statistical Computing. (Computing, R. F. f. S. ed., Vienna, Austria
19. Wettenhall, J. M., Simpson, K. M., Satterley, K., and Smyth, G. K. (2006) *Bioinformatics* **22**, 897-899
20. Wu, Z., and Irizarry, R. A. (2004) *Nat Biotechnol* **22**, 656-658; author reply 658
21. Storey, J. D., and Tibshirani, R. (2003) *Proc Natl Acad Sci U S A* **100**, 9440-9445

22. Breitkreutz, B. J., Stark, C., and Tyers, M. (2003) *Genome Biol* **4**, R22
23. Mendes, N. D., Casimiro, A. C., Santos, P. M., Sa-Correia, I., Oliveira, A. L., and Freitas, A. T. (2006) *Bioinformatics* **22**, 2996-3002
24. Monteiro, P. T., Mendes, N. D., Teixeira, M. C., d'Orey, S., Tenreiro, S., Mira, N. P., Pais, H., Francisco, A. P., Carvalho, A. M., Lourenco, A. B., Sa-Correia, I., Oliveira, A. L., and Freitas, A. T. (2008) *Nucleic Acids Res* **36**, D132-136
25. Pfaffl, M. W. (2001) *Nucleic Acids Res* **29**, e45
26. Pfaffl, M. W., Horgan, G. W., and Dempfle, L. (2002) *Nucleic Acids Res* **30**, e36
27. Derkatch, I. L., Bradley, M. E., Zhou, P., Chernoff, Y. O., and Liebman, S. W. (1997) *Genetics* **147**, 507-519
28. Reimers, M., and Carey, V. J. (2006) *Methods Enzymol* **411**, 119-134
29. Huang da, W., Sherman, B. T., and Lempicki, R. A. (2009) *Nat Protoc* **4**, 44-57
30. Manogaran, A. L., Fajardo, V. M., Reid, R. J., Rothstein, R., and Liebman, S. W. (2010) *Yeast* **27**, 159-166
31. Kassir, Y., Adir, N., Boger-Nadjar, E., Raviv, N. G., Rubin-Bejerano, I., Sagee, S., and Shenhar, G. (2003) *Int Rev Cytol* **224**, 111-171
32. Kadosh, D., and Struhl, K. (1997) *Cell* **89**, 365-371
33. Carrozza, M. J., Florens, L., Swanson, S. K., Shia, W. J., Anderson, S., Yates, J., Washburn, M. P., and Workman, J. L. (2005) *Biochim Biophys Acta* **1731**, 77-87; discussion 75-76
34. Willingham, S., Outeiro, T. F., DeVit, M. J., Lindquist, S. L., and Muchowski, P. J. (2003) *Science* **302**, 1769-1772
35. Collins, S. R., Kemmeren, P., Zhao, X. C., Greenblatt, J. F., Spencer, F., Holstege, F. C., Weissman, J. S., and Krogan, N. J. (2007) *Mol Cell Proteomics* **6**, 439-450
36. Gavin, A. C., Aloy, P., Grandi, P., Krause, R., Boesche, M., Marzioch, M., Rau, C., Jensen, L. J., Bastuck, S., Dumpelfeld, B., Edelmann, A., Heurtier, M. A., Hoffman, V., Hoefert, C., Klein, K., Hudak, M., Michon, A. M., Schelder, M., Schirle, M., Remor, M., Rudi, T., Hooper, S., Bauer, A., Bouwmeester, T., Casari, G., Drewes, G., Neubauer, G., Rick, J. M., Kuster, B., Bork, P., Russell, R. B., and Superti-Furga, G. (2006) *Nature* **440**, 631-636
37. Grandi, P., Rybin, V., Bassler, J., Petfalski, E., Strauss, D., Marzioch, M., Schafer, T., Kuster, B., Tschochner, H., Tollervey, D., Gavin, A. C., and Hurt, E. (2002) *Mol Cell* **10**, 105-115
38. Wyttenbach, A., Swartz, J., Kita, H., Thykjaer, T., Carmichael, J., Bradley, J., Brown, R., Maxwell, M., Schapira, A., Orntoft, T. F., Kato, K., and Rubinsztein, D. C. (2001) *Hum Mol Genet* **10**, 1829-1845
39. Sipione, S., Rigamonti, D., Valenza, M., Zuccato, C., Conti, L., Pritchard, J., Kooperberg, C., Olson, J. M., and Cattaneo, E. (2002) *Hum Mol Genet* **11**, 1953-1965
40. Crocker, S. F., Costain, W. J., and Robertson, H. A. (2006) *Brain Res* **1088**, 176-186
41. Runne, H., Regulier, E., Kuhn, A., Zala, D., Gokce, O., Perrin, V., Sick, B., Aebischer, P., Deglon, N., and Luthi-Carter, R. (2008) *J Neurosci* **28**, 9723-9731
42. Doumanis, J., Wada, K., Kino, Y., Moore, A. W., and Nukina, N. (2009) *PLoS One* **4**, e7275
43. Hinnebusch, A. G. (1984) *Proc Natl Acad Sci U S A* **81**, 6442-6446
44. Hinnebusch, A. G. (1997) *J Biol Chem* **272**, 21661-21664

45. Steffen, K. K., MacKay, V. L., Kerr, E. O., Tsuchiya, M., Hu, D., Fox, L. A., Dang, N., Johnston, E. D., Oakes, J. A., Tchao, B. N., Pak, D. N., Fields, S., Kennedy, B. K., and Kaeberlein, M. (2008) *Cell* **133**, 292-302
46. Lu, P. D., Harding, H. P., and Ron, D. (2004) *J Cell Biol* **167**, 27-33
47. Mascarenhas, C., Edwards-Ingram, L. C., Zeef, L., Shenton, D., Ashe, M. P., and Grant, C. M. (2008) *Mol Biol Cell* **19**, 2995-3007
48. Matsuo, R., Kubota, H., Obata, T., Kito, K., Ota, K., Kitazono, T., Ibayashi, S., Sasaki, T., Iida, M., and Ito, T. (2005) *FEBS Lett* **579**, 2433-2438
49. Tain, L. S., Mortiboys, H., Tao, R. N., Ziviani, E., Bandmann, O., and Whitworth, A. J. (2009) *Nat Neurosci* **12**, 1129-1135
50. Zid, B. M., Rogers, A. N., Katewa, S. D., Vargas, M. A., Kolipinski, M. C., Lu, T. A., Benzer, S., and Kapahi, P. (2009) *Cell* **139**, 149-160
51. King, M. A., Hands, S., Hafiz, F., Mizushima, N., Tolkovsky, A. M., and Wyttenbach, A. (2008) *Mol Pharmacol* **73**, 1052-1063
52. Yeger-Lotem, E., Riva, L., Su, L. J., Gitler, A. D., Cashikar, A. G., King, O. D., Auluck, P. K., Geddie, M. L., Valastyan, J. S., Karger, D. R., Lindquist, S., and Fraenkel, E. (2009) *Nat Genet* **41**, 316-323
53. Liang, J., Clark-Dixon, C., Wang, S., Flower, T. R., Williams-Hart, T., Zweig, R., Robinson, L. C., Tatchell, K., and Witt, S. N. (2008) *Hum Mol Genet* **17**, 3784-3795

FOOTNOTES

F.G. is supported by the Medical Research Council, the CHDI Foundation, and the Huntington's Disease Association. P.J.M. is supported by National Institute of Neurological Disease Grant NS47237. T.F.O. is supported by EMBO and Marie Curie IRG. L.M. is supported by the Fundação para a Ciência e a Tecnologia (FCT). We would like to thank M. Sherman and A. Meriin for the pYES2-Htt25Q and pYES2-Htt103Q constructs.

The abbreviations used are: HD – Huntington's disease; htt – huntingtin; polyQ – polyglutamine; ROS – reactive oxygen species; KMO – kynurenine 3-monooxygenase; 3-HK – 3-hydroxykynurenine; QUIN – quinolinic acid; HDAC – histone deacetylase; TBP – TATA-binding protein; RPL - ribosomal protein, large subunit; RPS ribosomal protein, small subunit; DEG – differentially expressed gene; GO – gene ontology.

FIGURE LEGENDS

Fig. 1. Identification of DEGs in wild-type and gene deletion suppressor strains expressing Htt103Q. (A) Volcano plot of DEGs. The log2 of the fold change (Htt103Q versus Htt25Q) is represented on the x-axis and the negative log of P-values from t-test analyses is represented on the y-axis. Up-regulated genes due to Htt103Q have positive fold-changes. Red indicates DEGs at the FDR of $q < 0.1$, orange indicates $0.1 < q < 0.2$, and blue indicates $q > 0.2$. (B) Venn diagram indicating the overlap in DEGs between *bna4*Δ *mbf1*Δ, and *ume1*Δ strains expressing Htt103Q compared to the parental BY4741 strain. 15 DEGs are shared among the three deletion strains. (C) Inverse correlation of log fold change (M) in DEGs in suppressors expressing Htt103Q on the y-axis and in a wild-type strain expressing Htt103Q (compared with Htt25Q-expressing cells) on the x-axis. Blue: *bna4*Δ ($r=-0.77$, $t = -4.19$, $df = 12$, $P < 0.01$), Red: *mbf1*Δ ($r= -0.74$, $t = -4.10$, $df = 14$, $P = 0.01$), Green: *ume1*Δ ($r=-0.67$, $t = -4.84$, $df = 29$, $P < 0.0001$).

Fig. 2. Rnq1p is present in prion conformation in gene deletion suppressor strains. [RNQ^+] prion status in wild-type yeast and deletion suppressors (BY4741 parental strain) carrying the pYES2 empty vector or

expressing Htt103Q was determined by a combination of high-speed centrifugation and immunoblotting. "T" indicates total extract for each yeast strain, while "S" indicates supernatant fraction (soluble form of Rnq1), and "P" indicates pellet fraction (prion form of Rnq1, [RNQ^+]). (A) Immunoblotting with α-Rnq1 antibody showed that Rnq1 is found exclusively in the pellet fraction of the BY4741 wild-type strain, as well as the *mbf1*Δ and *ume1*Δ strains, indicating the protein is in the prion conformation. (B) In the BY4741 *bna4*Δ strain, [RNQ^+] prion status is "mixed", with protein present in both pellet and supernatant fractions. Treatment of BY4741 *bna4*Δ and parental cells carrying pYES2 with guanidine hydrochloride (GuHCL) cures [RNQ^+] prion, shifting Rnq1p from the pellet fraction to the supernatant fraction. (C) [RNQ^+] prion status is independent of *BNA4* deletion. In Y5563 *bna4*Δ cells all Rnq1 is found in the pellet fraction. Treatment of Y5563 *bna4*Δ cells with GuHCL cured [RNQ^+] prion present in the pellet fraction of untreated cells carrying pYES2, moving Rnq1 to the supernatant fraction.

Fig. 3. Suppression of Htt103Q toxicity in yeast overexpression strains. Parental wild-type Y258 yeast containing constructs for the overexpression of the indicated yeast ORFs were transformed with p425-Htt25Q or p425-Htt103Q and cellular viability determined using growth assays. The expression of both the huntingtin constructs and the indicated yeast ORFs is induced by galactose. Five-fold serial dilutions starting with equal number of cells of the four representative ORF suppressors are shown.

Fig. 4. Network analysis uncovers a high degree of interconnectivity amongst functionally validated DEGs. Osprey network analysis of 14 DEGs (indicated in bold) which suppress toxicity of Htt103Q when overexpressed. All interactions for these genes (both physical and genetic) were included in the analysis. Genes described by the same significantly enriched GO terms are color-coded and grouped together. Network data analyzed with an iterative minimum filter of 2 (minimum of 2 interactions with other network genes). A total of 81 nodes and 156 edges define this network, which contains 11 of the original 14 functionally validated genes.

Table 1. Common DEGs between *bna4*Δ, *mbf1*Δ, and *ume1*Δ suppressor strains expressing Htt103Q as compared to the parental BY4741 wild-type strain**.**

Gene	Htt103Q	*bna4*Δ	*mbf1*Δ	*ume1*Δ	Function
ANB1	n/c	Up	Up	Up	Translation elongation factor eIF-5A
AQR1	Down	Up	Up	Up	Plasma membrane multidrug transporter
COS7	Up	Up	Up	Down	Mitochondrial protein of unknown function
DAK2	Up	Down	Down	Down	Dihydroxyacetone kinase
DIP5	n/c	Up	Up	Up	Dicarboxylic amino acid permease
DLD3	n/c	Up	Up	Up	D-lactate dehydrogenase,
LYS20	n/c	Up	Up	Up	Homocitrate synthase isozyme
MMP1	n/c	Up	Up	Up	High-affinity S-methylmethionine permease
SPG4	Up	Up	Down	Down	Protein required for survival at high temperatures
SUF2	n/c	Down	Down	Down	tRNA-Pro, 1 of 3 nuclear tRNAs; anticodon AGG
SUF10	n/c	Down	Down	Down	tRNA-Pro, 1 of 3 nuclear tRNAs; anticodon AGG
TK(CUU)J	n/c	Down	Down	Down	tRNA-Lys, imported into mitochondria; AAG
YGR035C	Down	Up	Up	Up	Protein of unknown function, Cdc28 substrate
YMC2	Down	Up	Up	Up	Mitochondrial inner membrane transporter
YOR338W	Down	Up	Up	Up	Protein of unknown function; regulated by Azf1

Shaded areas indicate genes differentially expressed in all three suppressor strains, as well as in Htt103Q-expressing parental cells (in the opposite direction). Htt103Q differential expression is related to Htt25Q-expressing parental cells ($q < 0.2$). DEGs in the three suppressor strains expressing Htt103Q (*bna4*Δ, *mbf1*Δ, and *ume1*Δ are relative to parental cells expressing Htt103Q (top 200 annotated genes, $q < 0.1$).

Table 2. Families of over-represented motifs in promoter regions of genes differentitally expressed in Htt103Q versus Htt25Q yeast cells.

Family	Count*	P-value	Transcription factors**
TTTATAT	26	1.77e-06	Mig2p, Hap1p, Fzf1p, Zap1p
TTCTTTTC	17	3.59e-06	Azf1p, Cup2p, Zap1p, Ime1p
AAAAGAAA	22	9.24e-06	Azf1p, Zap1p, Cup2p, Tec1p
CATCGC	22	3.33e-05	Hap1p, Rfx1p, Ime1p, Rox1p,
GCGATG	22	3.33e-05	Hap1p, Rfx1p, Ime1p, Rox1p
CGCACA	21	0.000104	Crz1p, Hap1p, Aft2p, Stp2p
TGTGCG	21	0.000104	Crz1p, Aft2p, Stp2p, Hap1p
AAGAAG	39	0.000146	Tec1p, Azf1p, Zap1p, Azf1p
ATATTAT	24	0.000166	Arg81p, Arr1p, Mig1p,Mig3p
TTCTTC	39	0.000257	Tec1p, Zap1p, Abf1p, Ime1p
GCACGT	18	0.000573	Gcn4p, Met4p, Mig3p, Pho4p
ACGTGC	18	0.000573	Gcn4p, Pho4p, Met4p, Mig1p
GCGGCT	16	0.000988	Ume6p, Abf1p, Mig2p, Mig3p
AGCCGC	16	0.000988	Ume6p, Stp1p, Mig1p, Stp2p

* Count represents the number of sequences containing at least one motif in the family (out of 46).
** Only top four matches are listed for each family.

Table 3. DEGs in Htt103Q expressing cells modulate mutant htt toxicity.

Suppressor	Ortholog(s)*	Expression**	Function
BUD23	+	Down	rRNA processing
CSE2	-	Up	RNA pol II transcription
DBP2	+	Down	rRNA processing
ENT3	+	Up	Golgi -endosome transport
IPI3	-	Down	rRNA processing
JJJ3	-	Down	HSP40 chaperone
NSA2	+	Down	rRNA processing
PRM7	-	Down	pheromone response
RAS1	+	Down	G-protein signaling
RRP9	+	Down	rRNA processing
UTP9	-	Down	rRNA processing
YOR1	+	Down	ABC transporter
Deletion Suppressor			
*mbf1*Δ	+	Up	transcriptional coactivator
Deletion Enhancer			
*apj1*Δ	+	Up	HSP40 chaperone

*Human orthologs determined via the Ensembl Genome Browser. Orthologs may be either 1-to-1, 1-to-many, or many-many. *BUD23*, *ENT3*, *NSA2*, *RRP9*, and *MBF1* have 1-to-1 orthologs in humans which could potentially be targeted for therapeutics. **Refers to direction of differential expression in Htt103 versus Htt25Q cells.

Figure 1

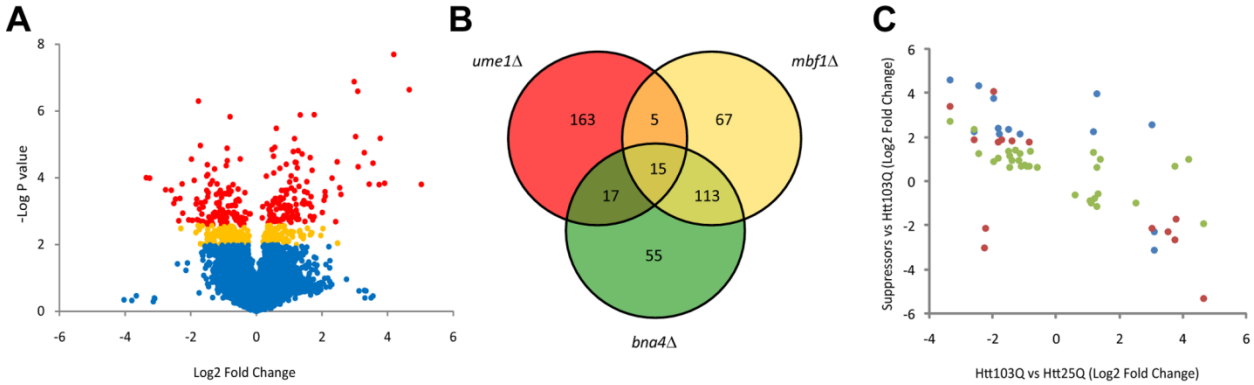
A
-Log P value
Log2 Fold Change
B
ume1Δ
mbf1Δ
bna4Δ
163
5
67
15
17
113
55
C
Suppressors vs Htt103Q (Log2 Fold Change)
Htt103Q vs Htt25Q (Log2 Fold Change)

Figure 2

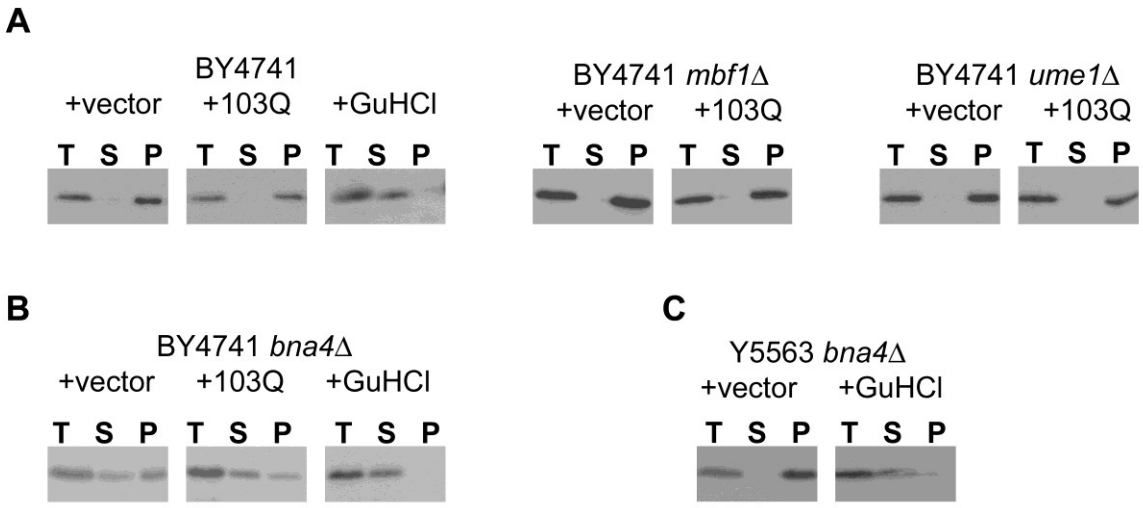
A
BY4741
+vector
+103Q
+GuHCl
T S P T S P T S P
BY4741 mbf1Δ
+vector
+103Q
T S P T S P
BY4741 ume1Δ
+vector
+103Q
T S P T S P
B
BY4741 bna4Δ
+vector
+103Q
+GuHCl
T S P T S P T S P
C
Y5563 bna4Δ
+vector
+GuHCl
T S P T S P

Figure 3

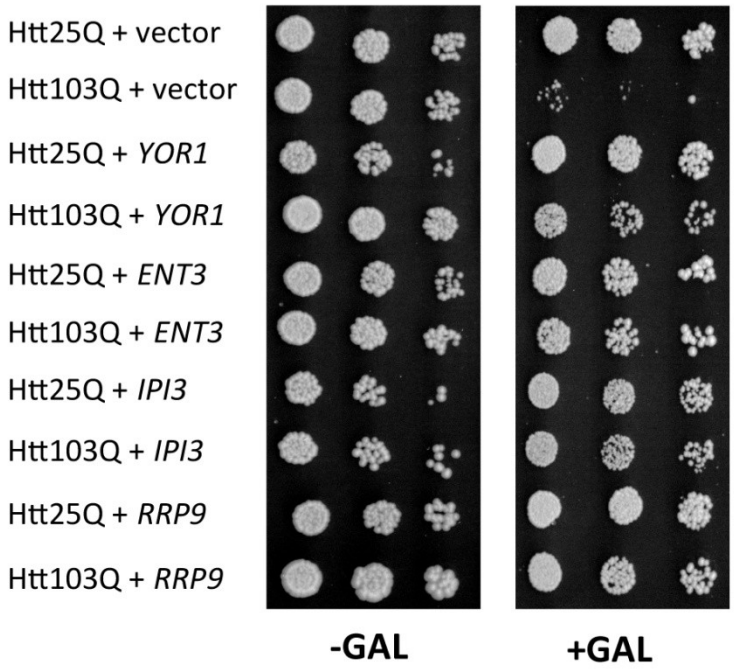
Htt25Q + vector
Htt103Q + vector
Htt25Q + *YOR1*
Htt103Q + *YOR1*
Htt25Q + *ENT3*
Htt103Q + *ENT3*
Htt25Q + *IPI3*
Htt103Q + *IPI3*
Htt25Q + *RRP9*
Htt103Q + *RRP9*
-GAL
+GAL

Figure 4

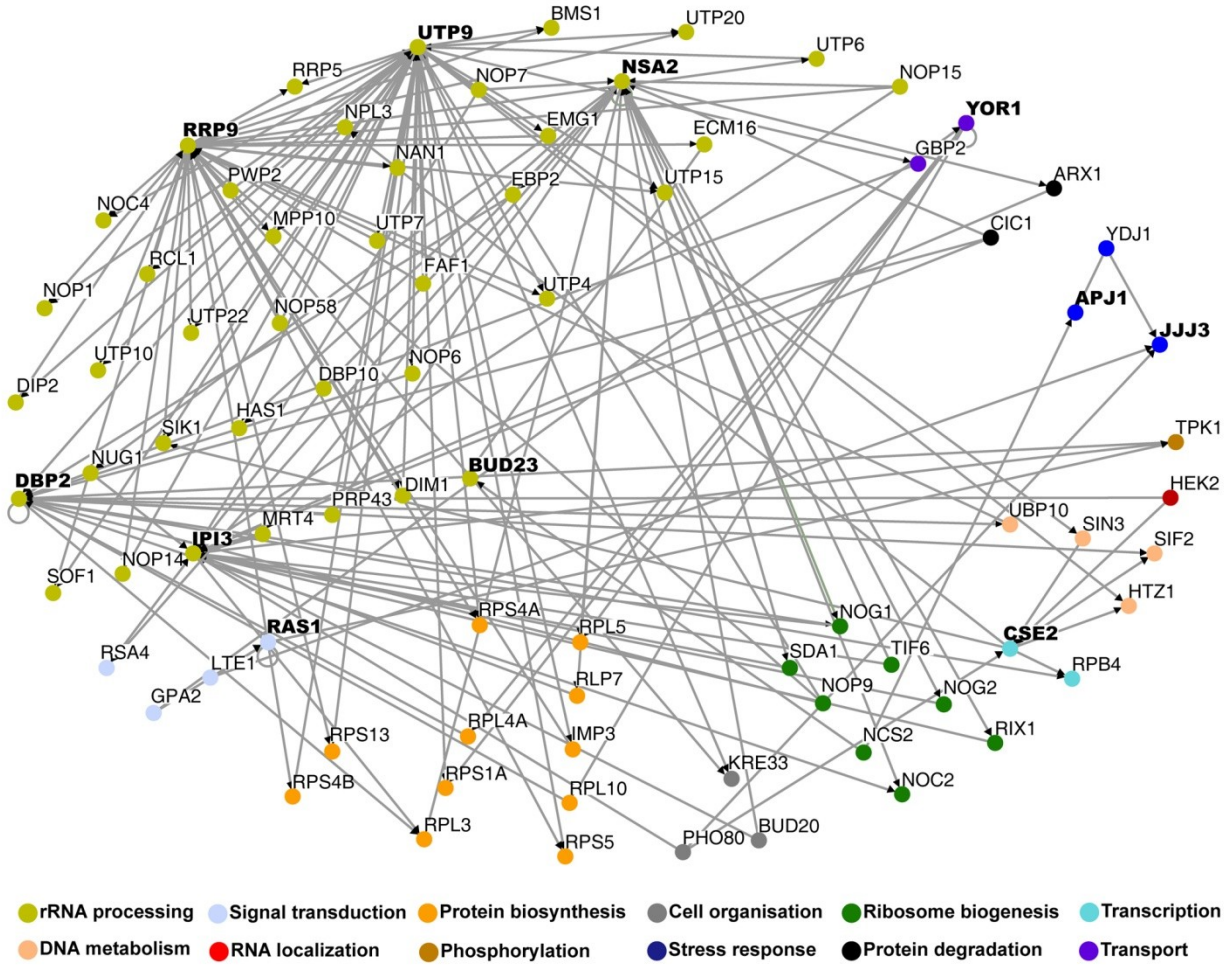
BMS1
UTP20
UTP9
UTP6
RRP5
NOP7
NSA2
NOP15
NPL3
YOR1
EMG1
ECM16
RRP9
NAN1
GBP2
PWP2
EBP2
UTP15
ARX1
NOC4
MPP10
UTP7
CIC1
YDJ1
RCL1
FAF1
NOP1
UTP4
APJ1
UTP22
NOP58
JJJ3
UTP10
NOP6
DBP10
DIP2
HAS1
SIK1
TPK1
NUG1
BUD23
DBP2
DIM1
HEK2
PRP43
UBP10
MRT4
SIN3
IPI3
SIF2
NOP14
SOF1
HTZ1
RPS4A
NOG1
RAS1
RPL5
CSE2
RSA4
SDA1
TIF6
LTE1
RPB4
RLP7
NOP9
NOG2
GPA2
RPS13
RPL4A
IMP3
NCS2
RIX1
KRE33
RPS1A
NOC2
RPS4B
RPL10
RPL3
PHO80
BUD20
RPS5
rRNA processing
Signal transduction
Protein biosynthesis
Cell organisation
Ribosome biogenesis
Transcription
DNA metabolism
RNA localization
Phosphorylation
Stress response
Protein degradation
Transport